

Review

Review of sEMG for Robot Control: Techniques and Applications

Tao Song^{1,2}, Zhe Yan^{1,*}, Shuai Guo^{1,3}, Yuwen Li¹, Xianhua Li⁴ and Fengfeng Xi⁵

- ¹ Shanghai Key Laboratory of Intelligent Manufacturing and Robotics, School of Mechatronic Engineering and Automation, Shanghai University, Shanghai 200444, China; songtao43467226@shu.edu.cn (T.S.)
- ² Shanghai Golden Arrow Robot Technology Co., Ltd., 701, Building 3, No. 377 Shanlian Road, Baoshan District, Shanghai 200444, China
- ³ National Demonstration Center for Experimental Engineering Training Education, Shanghai University, Shanghai 200444, China
- ⁴ School of Artificial Intelligence, Anhui University of Science and Technology, Huainan 232001, China
- ⁵ Department of Aerospace Engineering, Toronto Metropolitan University, 350 Victoria Street, Toronto, ON M5B 2K3, Canada
- * Correspondence: yanz@shu.edu.cn

Abstract: Surface electromyography (sEMG) is a promising technology that can capture muscle activation signals to control robots through novel human–machine interfaces (HMIs). This technology has already been applied in scenarios such as prosthetic design, assisted robot control, and rehabilitation training. This article provides an overview of sEMG-based robot control, covering two important aspects: (1) sEMG signal processing and classification methods and (2) robot control strategies and methods based on sEMG. First, the article outlines the general steps in sEMG signal processing and summarizes the commonly used methods for data acquisition, pre-processing, and feature extraction. In addition, machine-learning-based pattern recognition methods have been introduced for sEMG signal classification. Subsequently, user intent-based robot control strategies are classified into three categories: full-human continuous control, semi-autonomous continuous control, and discrete control, and their control methods and applicable scenarios are compared. Finally, this article discusses the advantages, disadvantages, and future development prospects of sEMG-based robot control. This review provides a comprehensive overview of sEMG-based robot control, from signal processing and classification methods to robot control strategies and methods, aiming to guide future research on selecting filters, feature sets, and pattern recognition methods and to assist in establishing sEMG-driven robot control frameworks.

Keywords: sEMG; signal processing; pattern recognition; robot control; rehabilitation



Citation: Song, T.; Yan, Z.; Guo, S.; Li, Y.; Li, X.; Xi, F. Review of sEMG for Robot Control: Techniques and Applications. *Appl. Sci.* **2023**, *13*, 9546. <https://doi.org/10.3390/app13179546>

Academic Editor: Dimitris Mourtzis

Received: 5 July 2023

Revised: 17 August 2023

Accepted: 19 August 2023

Published: 23 August 2023



Copyright: © 2023 by the authors. Licensee MDPI, Basel, Switzerland. This article is an open access article distributed under the terms and conditions of the Creative Commons Attribution (CC BY) license (<https://creativecommons.org/licenses/by/4.0/>).

1. Introduction

Surface electromyography (sEMG) is the superposition of numerous motor unit action potentials (MUAPs) in time and space, which can be recorded by sEMG sensors. sEMG-based technologies have been widely used in rehabilitation [1–7], exercise physiology [8–10], and other fields [11–15]. Research by Das Deutsche Zentrum für Luft- und Raumfahrt (DLR) has shown that, among various biological signal interfaces in the design of HMIs, non-invasive methods in BCI (brain–computer interface technology, including electroencephalograms, magnetoencephalography, and functional magnetic resonance imaging) have poor time or spatial resolution, whereas invasive methods (electrocorticography and microelectrodes) perform well but have harsh usage conditions, making them unfeasible for robot control [16]. There have also been studies that explore the use of head, tongue, and eye movements as control signals [17]; however, these methods are difficult to apply to the continuous control of robotic arms. With the gradual maturity of sEMG sensor

technology, the convenience and practicality of using sEMG in device control has become increasingly prominent.

The sEMG signal, which appears 50–100 ms before movement [18,19], can be used to predict human movement and then control robots based on such predictions. There are numerous application scenarios for sEMG-based robot control. In the rehabilitation field, Lu created an EMG-driven exoskeleton hand robot designed to assist in hand rehabilitation training of neurologically injured patients [20]. Sun demonstrated the effectiveness of sEMG-driven robots in stroke rehabilitation training [7]. Secciani presented a fully wearable Hand Exoskeleton System (HES) controlled by a novel sEMG-based classification strategy [21]. It can also be used as an auxiliary device to assist individuals with limb movement impairment in their daily activities. Li introduced two novel strategies for power-assist exoskeleton control using sEMG [22]. Kiguchi has been working on sEMG-based neuro-fuzzy control in a power-assisted upper-limb exoskeleton [23]. Hagengruber and Vogel used sEMG as an interface to control a manipulator that can assist people with severe muscular atrophy (SMA) in some daily activities [24]. An integrated system with 27-DOF named EDAN consists of a wheelchair, a manipulator, and a robot hand and can help people with movement disorders in daily activities [25]. For amputees, some sEMG-driven prostheses are available [26,27]. The mode of robot control varies depending on the type of robot and application scenario. A method combining a low-pass filter with spherical linear interpolation was used for lightweight robot trajectory generation in Roman's study. Guided by an sEMG signal, the robot can mimic human motion with a small delay [28].

Despite extensive research on sEMG in the academic community, its development in practical applications, particularly in robot control, is not yet mature. Factors such as instability and interindividual variability of sEMG signals pose significant challenges for control. A comprehensive review of the relevant literature will be constructive in synthesizing key research results and revealing major research trends in this field. Therefore, this study aimed to summarize and answer the following questions:

- What methods are used in each step of sEMG signal processing?
- What are the strategies and methods for robot control driven by sEMG?
- What are the advantages and disadvantages of using sEMG for robot control, the main challenges encountered, and the future development trends?

To address these questions, this paper searches for research articles, conference papers, and books related to the use of surface electromyography for robot control in the IEEE Xplore Digital Library, Web of Science, and PubMed databases using keywords such as sEMG, robot, exoskeleton, etc. that were published up to March 2023, with a focus on research on the use of surface electromyography for robot control in the past 10 years. Papers with unclear descriptions of research methods, low-quality reports, and review articles were excluded. The advantages and disadvantages of using sEMG for robot control are also discussed, along with the major challenges encountered and future development trends in this area. Overall, this review provides a valuable resource for researchers and practitioners in the field of sEMG-driven robot control.

2. Methods Summary in sEMG-Based Robot Control

Various methods have been used to process sEMG signals. In general, the processing steps are roughly the same: The signals are first filtered and amplified after collection. This step is crucial for subsequent research, especially for patient data where residual muscle strength may be weaker, meaning that their sEMG amplitude may be smaller by an order of magnitude or greater than that of healthy individuals. Therefore, reasonable filtering and amplification processes can ensure the signal-to-noise ratio of the signal, making it easier to extract sufficient motion information from sEMG. Feature extraction was then performed. Most studies focus on muscle activation levels; therefore, time-domain features are often selected for extraction. Studies related to muscle fatigue levels tend to focus on the frequency-domain features. In addition, there are studies based on time-frequency feature sets. Finally, sEMG signal recognition was performed, and various

machine-learning methods were used to decode the sEMG signals into limb movement information. This step is critical and is currently a research hotspot. Some scholars do not perform recognition; instead, they combine the muscle model proposed by Hill [29,30] to acquire muscle activation levels through sEMG and then perform subsequent research based on muscle activation. The main contents of this article are summarized in Figure 1.

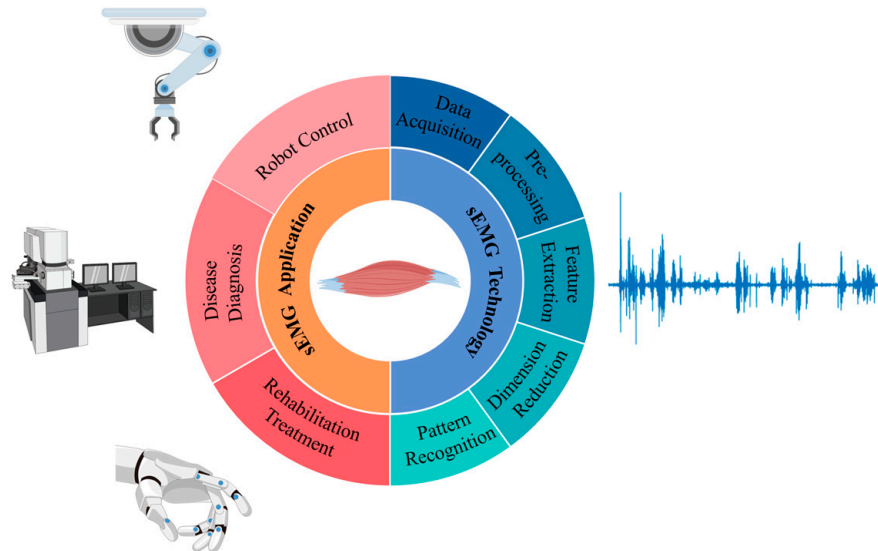


Figure 1. Summary of sEMG review (icons by Figdraw).

3. Processing and Pattern Recognition Methods

Raw sEMG signals cannot be applied to limb movement motion detection or robot control because of their spatial and time complexity. To obtain the subject’s movement information, sEMG signals need to be processed by data acquisition, pre-processing, feature extraction, dimensionality reduction (if necessary), and pattern recognition. Figure 2 provides an overview of the signal processing steps and methods. Data acquisition and pre-processing filter noise and signals emanating from unrelated muscles. The selection of the feature sets extracted from the processed signal is vital to the accuracy of the classifiers, which is the core of pattern recognition. The following paragraphs discuss the methods used in these steps.

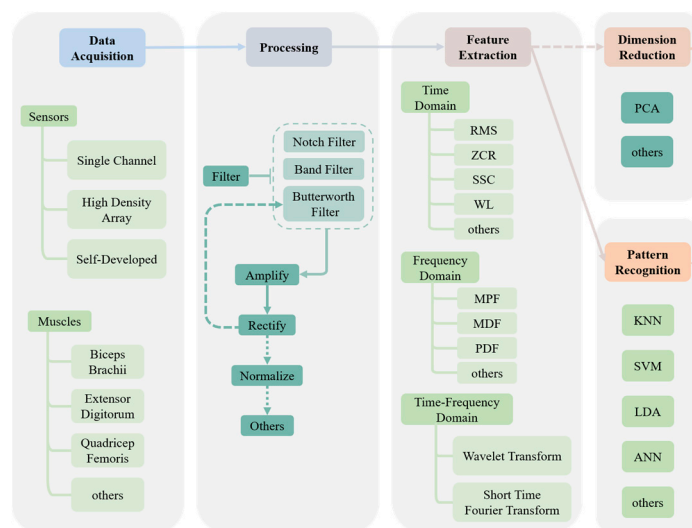


Figure 2. Processing and recognition methods of sEMG signals.

3.1. Data Acquisition

Many types of sEMG sensors have been applied in previous studies. Single-channel sEMG sensors focus on a particular area of muscle to try to eliminate the signals from uninterested muscles. This sensor is typically used in groups to form a multichannel acquisition system and simultaneously collect sEMG signals from different body parts. In contrast, high-density sEMG sensors can acquire spatial and temporal EMG information of a certain area using an electrode array that includes dozens of electrodes. Most researchers choose a commercial product that is quite mature compared with several self-made sensors. The Myo armband is a widely used product in hand gesture recognition based on sEMG [31–33]. Delsys Inc. provides various sensors for different situations [11,13,34,35]. In addition, some devices can provide biofeedback signals to stimulate the muscles of patients to help them perform rehabilitation exercises [36].

The knee, ankle, shoulder, elbow, wrist, and finger joints support most movements in activities of daily living. Therefore, muscles attached to the bones that make up these joints have been extensively studied for a long time. Table 1 shows the muscles of interest in some papers published in the last 20 years. From the table, it can be concluded that, for the upper limb, these muscles are the biceps brachii, triceps brachii, and deltoid; for the lower limb, the most interesting muscles are the quadriceps femoris, anterior tibial, and gastrocnemius; for the wrist and finger joints, these muscles mainly refer to the flexor/extensor carpi ulnaris/radialis and extensor digitorum. In addition, some authors have performed their work on other muscles of the human body. Wang studied speech recognition based on sEMG signals of the facial and neck muscles [13]. Potvin’s paper contributes to the load of the waist and abdomen muscles during repetitive weightlifting [12]. For studies in the field of hand gestures, the first dorsal interosseous, thenar, and hypothenar have also received attention from researchers.

Table 1. Summary of muscles of interest in sEMG studies.

Body Part	Joint	Muscles	References
Upper-limb	Hand gestures	flexor carpi radialis flexor carpi ulnaris flexor digitorum superficialis flexor digitorum profundus extensor digitorum first dorsal interosseous hypothenar extensor digiti minimi long palmar supinator abductor pollicis brevis	[6,31,33,37–72]
	Wrist	flexor carpi radialis extensor carpi radialis flexor carpi ulnaris extensor carpi ulnaris pronator teres extensor digitorum flexor digitorum	[16,22,24,37,38,73–79]

Table 1. Cont.

Body Part	Joint	Muscles	References
	Elbow	biceps brachii triceps brachii flexor carpi radialis extensor carpi radialis flexor carpi ulnaris extensor carpi ulnaris flexor digitorum superficialis brachioradialis brachialis anconeus pronator teres supinator extensor digitorum	[3,7,11,16,22–25,37,70,77,80–91]
	Shoulder	biceps brachii deltoid pectoralis major supraspinatus trapezius teres major teres minor infraspinatus latissimus dorsi	[9,22,23,37,75,80,82,84,86–88,91–93]
	Hip	gluteus maximus hamstring	[10]
Lower-limb	Knee	quadriceps femoris hamstring gastrocnemius anterior tibial	[5,34,80,94–99]
	Ankle	gastrocnemius anterior tibial peroneus longus extensor digitorum longus peroneus brevis	[2,4,6,34,100]
Other parts	Face	masseter muscle	[13]
	Abdomen	rectus abdominis	[80]
	Back	erector spinalis	[12,80]

To obtain a higher signal-to-noise ratio (SNR), references [6,20,101,102] carried out a strict experimental protocol: shaving off the hair on the limbs, polishing the skin of the target area with sandpaper, wiping it with an alcohol pad, and finally, applying the medical gel. The authors of these studies believe that these steps are necessary for collecting satisfactory data, but most scholars have not executed such tedious operations in their experiments. Although there are some differences in the experimental protocols, researchers should be able to reach a consensus that the position of the sEMG sensor should be relatively fixed in each experiment. To maintain the same position in different trials, reference [73] divided the subject's forearm into seven areas according to their body structure and marked them with different colors. Vogel indicated that a slight deviation of the electrode will lead to a significant impact on the experimental results, but for SMA patients, maintaining the exact location in every test is challenging [37].

3.2. Pre-Processing

The primary purpose of pre-processing is to obtain filtered signals. Generally, noise can be divided into six classes: electronic devices' inherent noise, ambient noise, motion artifacts, inherent instability of sEMG signals, electrocardiographic artifacts, and cross-talk

from muscles around the target area [100,103,104]. Although some artifacts and cross-talk have been avoided by selecting the electrode position and using a wireless transform, raw data acquired by the sEMG sensor still contain many noise signals.

The most helpful information from the sEMG signal is distributed in the frequency band of 0 Hz–500 Hz, and the primary energy is concentrated in 20 Hz–150 Hz [105]. Based on this fact, most studies have used band-pass filters, and the frequency band of filtering is 20 Hz–500 Hz. De Luca [106,107] and Beck [8,101,108–110]’s works are based on a broader frequency band from 20 Hz to 1750 Hz, whereas others focus on a narrow band. The Butterworth band-pass filter is the most popular filter. The main difference in those studies in which the Butterworth filter is used is its order. Bidirectional filters help prevent phase shifts that filters may introduce [42,51,77,92]. To eliminate the influence of power frequency interference on sEMG, a signal with a small amplitude, Kline [111] and Kuan [112] used a notch filter at 50 Hz or 60 Hz. On the contrary, some scholars believe that the notch filter filters the bioelectrical information in the corresponding frequency band; therefore, they did not use a notch filter [96]. In addition to placing electrodes on the target muscles, Schiel [113] and Kuan [112] also placed an extra sensor on the nearby inactive muscle as the resting signal channel. By subtracting the resting signal from the signals of each target channel, the baseline noise and cross-talk can be filtered. After the first round of filtering, a low-pass filter was used again in some studies because the contraction frequency of muscles in healthy people is low under normal conditions [12,32,42,86]. High-frequency (>10 Hz) nerve stimulation triggers tonic contraction of skeletal muscle, which is a concern of scholars who pay attention to Parkinson’s disease and stroke patients.

The power of the sEMG signal is meager, and the maximum amplitude is generally less than 10 mV [48]. Therefore, amplifying the sEMG signal is necessary to facilitate the signal acquisition. However, most acquisition systems can perform this step automatically, and researchers no longer need to handle it manually. The amplitude of the sEMG signals is assumed to be proportional to the muscle tension [48]. Thus, the strength difference between muscles (including individual differences) is inconvenient when comparing the effort levels during muscle contraction. In this case, normalization is beneficial. In addition to the above pre-processing methods, there are rectification, dimension reduction, and other methods. The pre-processing techniques used in related studies are summarized in Table 2.

Table 2. Summary of pre-processing, feature sets, and classifiers.

Reference	Pre-Processing *	Feature Sets **	Classifiers **	Publish Time
[4]	1-2-5	RMS, MAV	SVR	2014
[6]	2	logarithmic transferred time-domain features, traditional time-domain features	LDA, KNN, NaiveBayes	2017
[7]	1-2	fApEn	-	2014
[11]	-	WL, SSC, ZCR, AMP	Gauss Process	2021
[14]	2	RMS, MFR, MPF	-	2014
[18]	-	STFT, WPT	-	2014
[22]	-	RMS	Fuzzy, NN	2012
[24]	-	AMP, SSC, ZCR, WL	LDA	2018
[26]	2-5	MPF, MDF	-	2018
[27]	-	self-defined features	LDA, NaiveBayes, RF, KNN	2016
[32]	2-3-6	MAV, VAR, WL, HIST, CC, mDWT	MLP(ANN), SVM	2015
[37]	-	AMP, SSC, ZCR, WL	Gauss Process	2018

Table 2. Cont.

Reference	Pre-Processing *	Feature Sets **	Classifiers **	Publish Time
[38]	1-2	MAV, AR	Improved dynamic time-warping algorithm	2014
[40]	2	MAV, Reflection Coefficients, Histogram, RMS, Autoregressive coefficient, Variance, Willison amplitude, Modified Median Frequency, Modified Mean Frequency	DT, SVM, NN, NaiveBayes	2016
[43]	-	1-Time Domain 2-Enhanced Time Domain 3-NinaPro Features 4-SampEn, CC, RMS, WL	SVM, ANN, RF, KNN, LDA	2019
[44]	8	IEMG, MAV, SSI, RMS, LOG, VAR	KNN	2018
[46]	2	MAV, VAR, SSC, WL, MNF	Linear SVM	2021
[49]	-	MAV, ZC, SSC, WL, AR	LDA	2022
[50]	9	RMS, VAR, MAV, SD	ELM	2019
[51]	2	RMS, AR, WL, ZC	Linear Bayes	2017
[52]	1-2-3-5	RMS, WL, ZC, MNF, AR	SVM	2020
[54]	-	MAV, WL, RMS, AR, ZC, SSC	SVM, LDA, KNN	2019
[55]	-	RMS, MMAV, MMAVTP, MPF	SVM	2020
[57]	2-5	MAV, WL, ZC, SSC	SVM	2020
[59]	-	Spatiotemporal characteristics	MEMD, CRNN	2020
[60]	5-9	RMS	SVM	2008
[62]	2	VAR, ZC, iEMG, WAMP	-	2020
[64]	-	RMS	GRU-RNN	2021
[67]	3-6	-	ConvEMG, LSTM	2021
[68]	2	TDD-FT, SSD	-	2022
[69]	3	-	RF, SVM	2021
[70]	12	WPT	LDB	2007
[74]	9	MAV, ZC, SSC, WL, RMS	SVM	2020
[75]	5-9	WPT	SVM, BPNN	2020
[76]	3-5-8-9	RMS, bursting initial time, bursting duration, bursting area, and the maximum value	-	2013
[80]	3	RMS, Autocovariance function	NN, Fuzzy	2009
[81]	3-4-6-7	IAV, WL	-	2011
[82]	3-6-7	IAV, ZC, VAR, MDF	-	2010
[87]	-	RMS	Fuzzy, NN	2007
[93]	-	MAV	Fuzzy, NN	2004
[94]	2	STFT	-	2020
[95]	-	RMS, iEMG	LSTM, MLP	2020
[96]	2	RMS, WL, VR	-	2021
[97]	-	RMS, WL, SSI, MAV, VAR, LOG, SampEn	ESECW	2021
[98]	5-6-9	OMA self-defined features	ANN	2017
[99]	-	WPT-PCA	SUKF, NN	2020
[112]	2-5-9	-	Linear regression, SVM	2010
[113]	9	AMP, SSC, ZCR, WL	-	2020
[114]	-	iEMG, MAV, MMAV, VAR, WL, WAMP	KNN	2012
[115]	1-3-4-5	RMS, WL, ZC, IAV, SSC, AR	PCA, LDA; PCA, SVM; OFNDA, LDA; OFNDA, SVM	2013
[116]	-	SampEn, CC, RMS, WL	-	2013

Table 2. Cont.

Reference	Pre-Processing *	Feature Sets **	Classifiers **	Publish Time
[117]	-	RMS	Fuzzy, NN	2013
[118]	-	TD-VAR, RMS; FD-MF, MPF; EMD	The series splicing method Complex vector method	2022
[119]	-	FFT	CviT	2022
[120]	-	SampEn	-	2012

* The numbers 1–9 in the ‘pre-processing’ column in the table represent amplification, band-pass, low-pass, high-pass, notch filter, rectification, normalization, dimensionality reduction, and other methods, respectively.
** Please refer to the Abbreviations part for the explanation of the abbreviations appearing in the Feature Sets and Classifiers columns in the table.

3.3. Feature Extraction

Before feature extraction, the signal segmentation should first be determined. An overlapping window is the most widely used method; however, the window width and overlapping width are different. The width of the window directly affects the effectiveness of the feature extraction and delay time. The larger the window width, the more information will be obtained, and the less the deviation of the extracted features will be, but more computing time will be required. In references [121–123], for the first time, it was suggested that the maximum delay in a closed-loop real-time control system should be less than 300 ms. A delay time of 100 ms–250 ms is appropriate, and the classifier’s performance should precede the delay time.

For a specific classifier, the selection of the feature sets of the sEMG signals is the most important factor affecting its performance. Signal analysis generally includes Time Domain (TD), Frequency Domain (FD), Time-Frequency Domain (TFD) transformation, and entropy. TD features are used most frequently and are mainly for muscle effort or active-level analysis; FD features are primarily utilized to study the level of muscle fatigue. They can also be recruited as supplement features to form a feature set together with TD features to improve the accuracy of classification. TFD transforms such as Short-Time Fourier Transform (STFT), Fast Fourier Transform (FFT), and wavelet transform retain the TD and FD characteristics of a signal. However, there are few studies based on TFD, owing to its complexity and poor interpretability. Fifty groups of standard features were recruited from reference [116] to select the most robust single feature and feature set. TD, FD, TFD, and Entropy features were also included. Based on the Linear Discriminant Analysis (LDA) classifier, the feature sets with the best performance are the Sample Entropy (SampEn), Cepstrum Coefficient (CC), Root Mean Square (RMS), and Wave Length (WL). The feature sets used in these studies are listed in Table 2.

3.4. Pattern Recognition

The data obtained through the above processing should be input into a classifier for pattern recognition that can extract human actions from sEMG signals through machine-learning (ML) methods. The classifier can then be applied to specific scenes, such as HMIs or prosthesis control. Academic research has focused on the type of classifier used and how to improve the accuracy of classification. In recent studies, Support Vector Machines (SVMs), Linear Discriminant Analysis (LDA), K-Nearest Neighbor (KNN), Decision Trees (DTs), Random Forest (RF), the Hidden Markov Model (HMM), Bayesian Classifiers (BCs), Fuzzy Control (FC), Recurrent Neural Networks (RNNs), Convolutional Neural Networks (CNNs), and Artificial Neural Networks (ANNs) as well as their improved models have been used to identify sEMG.

The performance of different classifiers in different scenarios may vary significantly when using machine-learning methods. Therefore, in recent studies, researchers have used various methods to simultaneously compare and select those with better performance. After extracting six TD features from the same dataset, a SVM, LDA, and KNN were

used for classification in Hussein's work, with accuracy rates of 96.16%, 95.07%, and 88.33%, respectively. For the SVM, the RBF core achieves a higher accuracy than the linear method [54].

In [11,24], the collected sEMG signal was mapped to the control commands using a machine-learning approach based on a Gaussian Process, where a space velocity (three dimensions) and a binary trigger signal were decoded. Then, the LDA classifier was used to interpret the binary trigger signal from the training data.

DT, LibSVM, KNN, and NaiveBayes, which are supported by the open-source machine tool Weka, were compared in [40]. For LibSVM, a grid search algorithm tunes the best RBF kernel parameters. The other three classifiers used default parameters. The experimental results show that the four classifiers LibSVM, KNN, DT, and NaiveBayes achieved 96.16%, 94.02%, 76.18%, and 63.87% accuracy, respectively, in the intra-subject test.

In a study of sEMG-controlled upper-limb prostheses under force variation conditions, the average error rates of LDA, RF, NaiveBayes, and KNN ($k = 3$) for hand gesture recognition were 17.42%, 17.97%, 19.07%, and 19.14%, respectively [27].

Long Short-Term Memory (LSTM) has been applied to gait phase recognition in a low-cost system [95]. LSTM has been used to solve the problem of long-term dependence in general RNNs since it was designed. It can effectively transfer and express information in a long time series without causing useful information to be ignored (forgotten). Simultaneously, LSTM can solve the problem of gradient disappearance/explosion in RNNs. The proposed method achieved average classification accuracies of 94.10%, 87.25%, 90.71%, 94.02%, and 87.87%, respectively, for different gaits. In addition, the proposed system exhibits an advantage in terms of real-time performance, with a low average time consumption.

Reference [34] worked on daily activity monitoring and fall detection based on sEMG and an accelerometer (ACC). The two signals were input into double-stream HMMs, a double stochastic process including Markov chains and a general stochastic process. $O = \{O^E, O^A\}$ is the model of the two-stream feature sequences, where O^E denotes the sEMG signals, and O^A denotes the ACC signals. The corresponding parameters of the two models, such as the transition probability matrix and observation probability distribution, were obtained through model training. The experimental results for 387 activities showed that the HMM achieved an average recognition accuracy of 98.3%.

Kiguchi's research [23,76,85,87,91,93,117] focused on applying neuro-fuzzy theory to control a power-assist exoskeleton of the upper limbs. In [23], the authors established a 4×12 mapping matrix between the RMS of a 12-channel sEMG and a 4-DOF upper limb (shoulder and elbow) motion. Each element in this matrix is the weight of each channel signal to 4-DOF torque. The neuro-fuzzy model is used to modify the weight value in the matrix so that the weight value can consider the influence of upper-limb posture and adapt to individual differences. The four joint angles were the inputs of the neuro-fuzzy modifier. After calculating the fuzzifier, rule, and defuzzifier layers, the weights were modified. The experimental results show that the model can effectively reduce the force level of users when they operate the exoskeleton.

Elahe proposed a novel deep architecture, referred to as XceptionTime, which integrates depth-wise separable convolutions, adaptive average pooling, and a new non-linear normalization technique. By connecting these modules in a series, XceptionTime can extract both temporal and spatial messages without the need for data augmentation or manual feature extraction. In addition, this model is more robust to input, less complex, and less likely to overfit. Based on the Nina dataset, DB1, the result indicates a better performance than other methods [124].

3.5. Datasets

Generally, the specific fields of research are different, and most researchers have conducted unique experiments on their topics. Thus, the datasets in different studies are quite different and are not universal. However, studies on biceps brachii, triceps brachii,

and hand gesture-related muscles are more popular. Some authors have contributed to open-source datasets of these muscles for future work.

Jarque-Bou provides a database of kinematics and sEMG of the forearm and hand, called the KIN-MUS UJI Dataset, recording 572 forearm angles and muscle activities of 22 subjects during activities of daily living [73]. The sEMG and Inertial Measurement Unit (IMU) signals of the forearm during typing, push-ups, weightlifting, and rest were collected using the Myo Thalmic band in Khan's study [53]. Al-Timemy AH provided EMG signals for patients with radial artery amputation for prosthetic control [27]. A dataset related to the hand movements of amputees provided in [125] can be used to study the relationship between the sEMG signal, hand kinematics, and hand force. Zhu used the Myo band to collect datasets under non-ideal conditions, including electrode displacement, individual differences, muscle fatigue, daytime differences, arm posture, and other factors, for robust research on the sEMG control system [66]. The literature [72] records 12 high-density sEMG signals of gestures for gesture recognition and the development of muscle-computer interfaces (MCIs). In [39], gesture recognition was based on the CapgMyo and CSLHDEMG datasets. Mónica provides a record of high-density EMG signals of five muscles of the upper limb [89]. Cene provides an open-source dataset of the upper limb for an Extreme Learning Machine (ELM) limit learning machine for intention detection [50]. Mohammed provided a method for simulating and generating EMG data from healthy individuals [114].

4. Application of sEMG Interface in Robot Control

The unique advantage of EMG in driving robots is its ability to capture bioelectric signals released during muscle contraction. The practicality, convenience, and earlier-than-movement characteristics of sEMG sensors also enable real-time control of robots. In the existing research, controlled robots are not limited to popular mechanical arms and exoskeletons. Wearable mechanical dexterous hands and gloves are also common in the rehabilitation field, and some scholars have studied the control of mobile robots, such as wheelchairs and wheeled robots. The control methods and difficulty levels vary for the different types of devices used in applications. In Section 4.1, we will discuss the differences in control strategies used in current research when the similarity between human motion and robot motion is different. In Section 4.2, we distinguish two methods for extracting human motion information from sEMG. These two different methods, combined with the three control strategies in Section 4.1, will form different robot control schemes.

4.1. Classification of Robot Control Strategies

The use of sEMG signals to drive robots or prosthetics can assist individuals with movement disorders in activities or enhance their movement abilities. Rehabilitation robots using neural interfaces have promising potential for the treatment of post-stroke patients. The control strategies for robots using sEMG interfaces can be generally categorized into full-human continuous control (S1), semi-autonomous continuous control (S2), and discrete control (S3). Their characteristics and related research are detailed in the following paragraphs.

4.1.1. Full-Human Continuous Control Strategy (S1)

Under this control strategy, the movement of the robot is entirely dependent on muscle activation information. The robot begins to move synchronously when the signal collected by the sEMG interface exceeds a given threshold. Typically, a robot's movement mimics human limb movement or collaborates with the subject to accomplish tasks when using this control strategy.

A Gaussian regression process-based method was used to control the manipulator in Vogel's study. They decoded biological signals using a Gaussian regression process and mapped an eight-channel sEMG to directed velocity-based 2D or 3D control commands for manipulator control in a microgravity (space) environment [11]. In [24,37], a machine-learning method based on the Gaussian regression process was used to transform the

EMG signals of SMA patients into force and velocity control commands for a manipulator. Weitschat proposed a spherical linear interpolation motion-planning method that allows an sEMG-controlled manipulator to imitate human motion with a short delay [28].

Artemiadis and Kyriakopoulos dimensionally reduced the acquired sEMG signals to two dimensions and mapped them to the four joint angles of the shoulder and elbow joints [82,86,88]. By interacting with a 4-DOF manipulator, the hand position and interaction force, which can be used as exoskeleton control, are obtained through the forward kinematics and dynamics of the human body.

Grafakos implemented variable admittance control for a 7-DOF manipulator based on sEMG and compared it with constant admittance control in terms of motion accuracy, execution time, and energy consumption [35]. Li implemented adaptive impedance control for an upper-limb exoskeleton using sEMG [126].

Fuzzy neural networks were used to model the various factors of the dominant muscles when the upper arm shoulder-elbow joint was in different positions in Kiguchi's work. The model takes multi-channel sEMG signals as input and maps them to the joint torques on the human upper limb. The resulting model is applied to control exoskeletons [23,76,85,87,91,93,117].

Li et al. collected sEMG information from agonist and antagonist muscles simultaneously to calculate the exoskeleton's joint torque control and applied LDA classifiers to improve the classification efficiency at each joint [22].

Liu et al. proposed a method to adapt a household rehabilitation bilateral exoskeleton's stiffness based on the user's dynamic motion using sEMG and upper-limb musculoskeletal models [3]. Ding proposed a model that combines Hill's muscle model and human dynamics to estimate the joint angular velocity and joint angle, which can be applied to drive a manipulator [81].

Sun et al. controlled a simple single-axis robot for upper-limb rehabilitation training for stroke patients using myoelectric signals from the triceps brachii [7]. Minatil proposed a control method for a 6-DOF robot that combines multi-sensor fusion perception and control, including eye tracking, EEG, EMG, and head motion sensors. This control method can be applied to control wheelchairs and daily assistive robots [127].

Zeng proposed an HRI method that combines both active and antagonist myoelectric signals to control a robotic gripper, allowing users to change grip stiffness by altering the degree of muscle contraction [49]. HRI can be applied to the remote operation of robots and the design of prosthetics. In [71], a hand synergistic control method combining a multifactor model and sEMG signals was proposed. A five-finger robotic hand with two degrees of freedom for each finger is illustrated in [69]. This robotic hand was driven by sEMG signals from the forearm, and control commands were generated by the classification results of EMG using the Random Forest (RF) method.

Khoshdel introduced a method that applies an ANN to estimate lower-limb strength from sEMG signals and apply it to a knee rehabilitation robot. Both human and robot models were simulated and experimentally validated using OpenSim [62,98]. In [4], a 6-DOF parallel robot was controlled by four channels of sEMG signals from the lower limb and applied to lower-limb rehabilitation. Fan used a fuzzy neural network to identify a user's motion intent based on sEMG and interactive forces [18]. The lower-limb exoskeleton robot uses the estimated human motion as the control command and feedback with the exoskeleton joint angle, forming a closed-loop rehabilitation system for human-machine collaboration. Malosio designed a spherical parallel 3-DOF robot for ankle-foot joint rehabilitation using sEMG and interactive force [2].

Kuan et al. combined binary intent estimation based on a SVM for sEMG classification and continuous intent estimation based on linear regression for force prediction for the control of a rehabilitation robot, which can help improve joint mobility in the human body [112]. Jain et al. studied an artificial finger that could perform biomimetic movements using sEMG signals from the index finger. This artificial finger was made of an ion-polymer metal composite material [128].

4.1.2. Semi-Autonomous Continuous Control Strategy (S2)

This strategy frequently requires a combination of many sensors, notably vision, for perception. The robot system follows the sEMG signal for movement and then uses signals from additional sensors to sense the surrounding environment and objects, further determining the user's motion intention and automatically executing a pre-programmed task template to aid in fulfilling the task.

Vogel provides shared control templates, which employ the subject's sEMG signals to direct the robotic arm's motion by combining visual perception from a camera with pre-set task action templates, such as drinking water, opening doors, and picking up objects. Based on this, the control computer infers the user's task intention and calls a shared control template for the robotic arm to aid the user in performing the task. During this procedure, the motion of the robotic arm is no longer solely determined by the sEMG signals [16,25,83].

Shenoy employs a different semi-automatic control method, extracting only the direction of movement from a recorded sEMG signal with a predefined speed and joint torque for the movement of a robotic arm [60]. Activation of the hand extensor and abductor pollicis brevis muscles controls the opening and closing of a wearable five-fingered mechanical hand with the motor moving at a constant angular velocity, as described in [42]. This artificial hand was utilized for hand rehabilitation training after a stroke.

4.1.3. Discrete Control Strategy (S3)

Unlike the previous two control strategies, in this strategy, the human and robot movements are often dissimilar. The most convenient and commonly used human movement involves various gestures, and there are studies using other limb movements of amputees. On the other hand, robot movements are expressed as movement or joint rotation, and there are more types of controllable devices. However, this type of control only uses sEMG signals for simple threshold control switch-label settings for specific movements. The control logic is simple but limited to simple scenarios involving few movements. For scenarios with many movements, a certain amount of learning is required.

Murillo defined five gestures as motion commands for a multi-axis mechanical arm, recorded sEMG signals using the Myo armband, identified them, and then controlled the mechanical arm to move in a predetermined manner [33]. Hassan collected EMG signals from the forearm using the Myo armband and compared the recognition accuracies of the SVM, LDA, and KNN algorithms [54]. The gesture recognition results were applied to control a mechanical arm with 5-DOF. In [31], the Myo armband was applied to recognize motions using sEMG and IMU signals, and the recognition results were used to control a PeopleBot home robot.

Chen mapped the sEMG signals of seven gestures to the movement and grasping of a mechanical arm, which matched seven predetermined movements [52]. The corresponding mechanical arm control commands were obtained from the results of SVM classification. Gowtham employed sEMG and IMU to control a 5-DOF mechanical arm, where the IMU signals of the left and right arms controlled the movement of four rotating DOF, and the sEMG signal of the palm opening and closing controlled the movement of the end gripper [129]. Abayasiri controlled the movement of electric wheelchairs and gripped mechanical arms using sEMG signals from both upper limbs [85]. Maeda developed eight wrist movements and mapped them using fuzzy logic for wheelchair motion commands [78].

Duan investigated the utilization of residual limb gestures of amputees for prosthesis control via EMG signals [65]. Shenoy et al. applied SVM classification to classify sEMG signals and mapped the results to four predetermined gestures, allowing a prosthetic robot to perform grabbing, left-right, up-and-down, and rotating movements [60]. AL-Quraishi et al. applied the results to the control of dexterous hand prostheses using sEMG signals from the forearms of amputees for motion classification recognition [6].

Lu et al. utilized four-channel sEMG signals from his forearm and hand to define six distinct actions and accomplished real-time control of a wearable five-finger robot for

hand mobility rehabilitation training [20]. Bisi et al. defined ten gestures and utilized the KNN algorithm for sEMG classification recognition, translating these into mobile robot control commands [44]. Tamilselvi et al. designed a simple mechanical arm for amputees that could be controlled by a sEMG interface for rudimentary movements [26]. Nam et al. proposed a human–machine interface based on the fusion of three sensors: glosso-kinetic potential, electrooculogram, and EMG signals from facial muscles, providing robot assistance for people with limb movement disorders or complete paralysis [17].

4.2. Robot Control Methods Using sEMG Interfaces

In the research mentioned in the previous section, the methods for translating sEMG signals into robot control commands can be divided into the following two categories:

Human Model-Based Method (M1): M1 involves solving muscle activation levels from sEMG data, estimating human motion based on musculoskeletal models and human dynamics, and commanding robots for human–robot collaboration activities or exoskeleton devices to follow human motion.

Machine-Learning-Based Method (M2): M2 considers the physical system of muscle-driven bone movement in the human body as a black box and uses machine-learning techniques to directly convert sEMG signals to the joint torque and joint angle. Then, the position, velocity, and force control are implemented based on the kinematics of the robot. Interestingly, Bu starts with processed sEMG pictures and uses the YOLO algorithm to identify joint movement and detect joint angles [79].

Figure 3 shows the relationship between control methods and control strategies. When using muscle signals from limb movement (arms or legs), most researchers employ the M1 or M2 approaches. Generally, more studies adopt the M2 than the M1. The reason for this, in the author’s opinion, is that human modeling based on physiology and biomechanics is highly complex, and it is difficult to guarantee its accuracy. In addition, this form of the model is easily affected by individual variances, leading to low generalizability. Hand gesture movements involve so many muscles and bones that it is difficult to discuss their dynamics. Hence, hand gesture-related research uses the machine-learning method M2 to make the process easier.

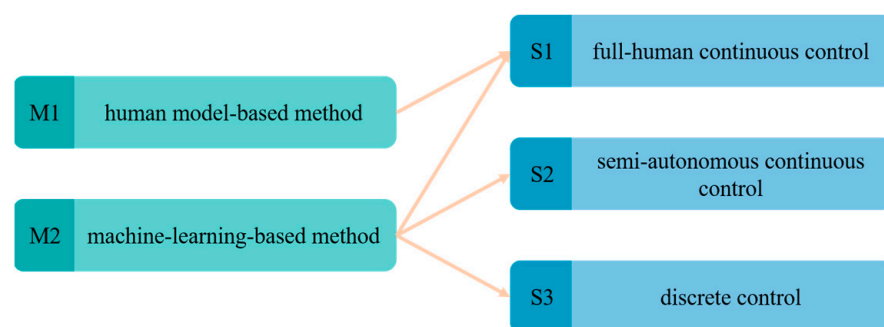


Figure 3. sEMG-driven robot control method and control strategy.

5. Discussion and Future Perspectives

sEMG signals contain rich information, which can not only reflect the level of muscle activation and the strength of contraction, but also extract information on limb movement control, limb impedance, and muscle fatigue. The use of sEMG sensors does not require complex operations, and signals can be obtained by attaching electrodes to the skin, which is simple, convenient, and efficient. sEMG precedes movement, which makes it advantageous as a control interface for devices, and it can be used to predict human motion in real time. The myoelectric signals of the residual muscle can still provide movement information for people with movement disorders or amputations.

However, there are still some unresolved challenges in using sEMG as a control signal for robotic arms. The information obtained from sEMG is ambiguous. The biological signals of adjacent muscles overlap and form cross-talk, making it difficult to extract

specific muscle information. Factors such as the electrode position and muscle fatigue during movement also affect the collected data. Differences between individuals, such as muscle development level and health status, mean the same control algorithm needs adjustment to its parameters to be applied to different people. There are few studies on individual differences, and the use of machine-learning methods to train with large sample sizes can reduce the negative effects of such differences to some extent.

After more than 20 years of research, pre-processing methods and the selection of signal feature sets for sEMG signals have matured. Currently, the research focuses mainly on the following two areas: one is the improvement and innovation of pattern recognition algorithms based on machine learning to achieve higher classification performance, mainly in terms of accuracy; the other is the design of new HMIs based on sEMG.

Many studies have been conducted on the use of sEMG for discrete robot control. These studies used supervised learning methods to map predefined actions onto the actions of the robot. Although this method is simple, its disadvantage is that the robot's movement capability is limited, and it can only perform several predetermined actions. Conversely, using sEMG to recognize continuous movement intentions and control the robot can greatly improve the flexibility of the controlled device; however, it is difficult to conduct theoretical research on the complex human muscle-bone model, which increases the difficulty of research.

In clinical medicine, sEMG can be used as biofeedback for the treatment of diseases such as Parkinson's disease and stroke. De Luca's research is dedicated to decomposing the obtained sEMG signal into motor unit action potentials (MUAP).

As an emerging technology, sEMG has been widely researched and applied in fields such as rehabilitation therapy, sports, and the design of new human-robot interactions. With the continuous progress of technology and the decrease in cost, the practicality, convenience, and uniqueness of sEMG sensors will mean they have good development prospects.

6. Conclusions

This study selected 129 relevant articles in the sEMG field over the past 20 years to summarize the research on sEMG signal processing methods, machine-learning-based sEMG pattern recognition methods, and sEMG-driven robot control methods and provide an overview of the advantages and disadvantages of using sEMG for robot control, as well as discuss the current research hotspots and challenges.

Owing to the different situations of subjects in various studies, as well as the different objects for signal acquisition and criteria for motion classification, it is of limited significance to directly compare the classification accuracy achieved in these experiments. This review does not include these in the table for comparison purposes.

Funding: This work was supported by the National Natural Science Foundation of China (82227807); the Shanghai Municipal of Science and Technology Commission (21SQBS00300); the Special fund for Digital Transformation of Shanghai (202202004); the Key Research and Development Program of Anhui Province (2022i01020015); and the Open Project of the Medical and Industrial Integration Laboratory of Jiangning Hospital Affiliated to Nanjing Medical University (JNYZXKY202218).

Institutional Review Board Statement: Not applicable.

Informed Consent Statement: Not applicable.

Data Availability Statement: Not applicable.

Conflicts of Interest: The authors declare no conflict of interest.

Abbreviations

Abbreviation	Complete Spelling
AMP	Amplitude
ANN	Artificial Neural Network
AR	Autoregressive Coefficient
BPNN	Back-Propagation Neural Network
CC	Cepstrum Coefficient
ConvEMG	Convolutional Electromyography
CRNN	Convolutional Recurrent Neural Network
CviT	Convolutional Vision Transformer
DT	Decision Tree
ELM	Extreme Learning Machine
EMD	Empirical Mode Decomposition
ESECV	Empirical Mode Filtering and Self-Enhancement Algorithm with Classical Wavelet
fApEn	Fuzzy Approximate Entropy
FD	Frequency Domain
FFT	Fast Fourier Transform
GRU	Gate Recurrent Unit
HIST	Histogram
IAV	Integral of Absolute Value
IEMG	Integrated Electromyography
KNN	K-Nearest Neighbor
LDA	Linear Discriminant Analysis
LDB	Local Discriminant Basis
LOG	Log Detector
LSTM	Long Short-Term Memory
MAV	Mean Absolute Value
MDF	Median Frequency
mDWT	Marginal Discrete Wavelet Transform
MEMD	Multivariate Empirical Mode Decomposition
MF	Mean Frequency
MFR	Mean Firing Rate
MLP	Multi-Layer Perceptron
MNF	Mean Frequency
MPF	Mean Power Frequency
NN	Neural Network
OFNDA	Orthogonal Fuzzy Neighborhood Discriminant Analysis
OMA	Online Moving Average
PCA	Principal Component Analysis
RF	Random Forest
RMS	Root Mean Square
RNN	Recurrent Neural Network
SampEn	Sample Entropy
SD	Standard Deviation
SSC	Slope Sign Change
SSD	Sum of Squares Difference
SSI	Simple Square Integral
STFT	Short-Time Fourier Transform
SUKF	Scale Unscented Kalman Filter
SVM	Support Vector Machine
SVR	Support Vector Regression
TD	Time Domain
VAR/VR	Variance
WL	Waveform Length
WPT	Wavelet Packet Transform
ZCR	Zero Cross Rate
ZC	Zero Cross

References

1. Neblett, R.; Gatchel, R.J.; Mayer, T.G. A Clinical Guide to Surface-EMG-Assisted Stretching as an Adjunct to Chronic Musculoskeletal Pain Rehabilitation. *Appl. Psychophysiol. Biofeedback* **2003**, *28*, 147–160. [[CrossRef](#)] [[PubMed](#)]
2. Malosio, M.; Negri, S.P.; Pedrocchi, N.; Vicentini, F.; Caimmi, M.; Molinari Tosatti, L. A Spherical Parallel Three Degrees-of-Freedom Robot for Ankle-Foot Neuro-Rehabilitation. In Proceedings of the 2012 Annual International Conference of the IEEE Engineering in Medicine and Biology Society, San Diego, CA, USA, 28 August–1 September 2012; IEEE: San Diego, CA, USA, 2012; pp. 3356–3359.
3. Liu, Y.; Guo, S.; Yang, Z.; Hirata, H.; Tamiya, T. A Home-Based Bilateral Rehabilitation System With SEMG-Based Real-Time Variable Stiffness. *IEEE J. Biomed. Health Inform.* **2021**, *25*, 1529–1541. [[CrossRef](#)] [[PubMed](#)]
4. Meng, W.; Ding, B.; Zhou, Z.; Liu, Q.; Ai, Q. An EMG-Based Force Prediction and Control Approach for Robot-Assisted Lower Limb Rehabilitation. In Proceedings of the 2014 IEEE International Conference on Systems, Man, and Cybernetics (SMC), San Diego, CA, USA, 5–8 October 2014; IEEE: San Diego, CA, USA, 2014; pp. 2198–2203.
5. Khoshdel, V.; Akbarzadeh, A. An Optimized Artificial Neural Network for Human-Force Estimation: Consequences for Rehabilitation Robotics. *IR* **2018**, *45*, 416–423. [[CrossRef](#)]
6. AL-Quraishi, M.S.; Ishak, A.J.; Ahmad, S.A.; Hasan, M.K.; Al-Qurishi, M.; Ghapanchizadeh, H.; Alamri, A. Classification of Ankle Joint Movements Based on Surface Electromyography Signals for Rehabilitation Robot Applications. *Med. Biol. Eng. Comput.* **2017**, *55*, 747–758. [[CrossRef](#)] [[PubMed](#)]
7. Sun, R.; Song, R.; Tong, K. Complexity Analysis of EMG Signals for Patients After Stroke During Robot-Aided Rehabilitation Training Using Fuzzy Approximate Entropy. *IEEE Trans. Neural Syst. Rehabil. Eng.* **2014**, *22*, 1013–1019. [[CrossRef](#)]
8. Stock, M.S.; Thompson, B.J. Effects of Barbell Deadlift Training on Submaximal Motor Unit Firing Rates for the Vastus Lateralis and Rectus Femoris. *PLoS ONE* **2014**, *9*, e115567. [[CrossRef](#)]
9. Swanson, B.T.; Holst, B.; Infante, J.; Poenitzsch, J.; Ortiz, A. EMG Activity of Selected Rotator Cuff Musculature during Grade III Distraction and Posterior Glide Glenohumeral Mobilization: Results of a Pilot Trial Comparing Painful and Non-Painful Shoulders. *J. Man. Manip. Ther.* **2016**, *24*, 7–13. [[CrossRef](#)]
10. McCurdy, K.; Walker, J.; Yuen, D. Gluteus Maximus and Hamstring Activation During Selected Weight-Bearing Resistance Exercises. *J. Strength. Cond. Res.* **2018**, *32*, 594–601. [[CrossRef](#)]
11. Hagengruber, A.; Leipscher, U.; Eskofier, B.M.; Vogel, J. Electromyography for Teleoperated Tasks in Weightlessness. *IEEE Trans. Hum.-Mach. Syst.* **2021**, *51*, 130–140. [[CrossRef](#)]
12. Potvin, J.R.; Norman, R.W.; McGill, S.M. Mechanically Corrected EMG for the Continuous Estimation of Erector Spinae Muscle Loading during Repetitive Lifting. *Europ. J. Appl. Physiol.* **1996**, *74*, 119–132. [[CrossRef](#)]
13. Wang, X.; Zhu, M.; Samuel, O.W.; Yang, Z.; Lu, L.; Cai, X.; Wang, X.; Chen, S.; Li, G. A Pilot Study on the Performance of Time-Domain Features in Speech Recognition Based on High-Density SEMG. In Proceedings of the 2021 43rd Annual International Conference of the IEEE Engineering in Medicine & Biology Society (EMBC), Guadalajara, Mexico, 1–5 November 2021; IEEE: Guadalajara, Mexico, 2021; pp. 19–22.
14. Trevino, M.A.; Herda, T.J.; Cooper, M.A. The Effects of Poliomyelitis on Motor Unit Behavior during Repetitive Muscle Actions: A Case Report. *BMC Res. Notes* **2014**, *7*, 611. [[CrossRef](#)]
15. De Luca, C.J. The Use of Surface Electromyography in Biomechanics. *J. Appl. Biomech.* **1997**, *13*, 135–163. [[CrossRef](#)]
16. Vogel, J.; Haddadin, S.; Jarosiewicz, B.; Simeral, J.D.; Bacher, D.; Hochberg, L.R.; Donoghue, J.P.; van der Smagt, P. An Assistive Decision-and-Control Architecture for Force-Sensitive Hand–Arm Systems Driven by Human–Machine Interfaces. *Int. J. Robot. Res.* **2015**, *34*, 763–780. [[CrossRef](#)]
17. Nam, Y.; Koo, B.; Cichocki, A.; Choi, S. GOM-Face: GKP, EOG, and EMG-Based Multimodal Interface With Application to Humanoid Robot Control. *IEEE Trans. Biomed. Eng.* **2014**, *61*, 453–462. [[CrossRef](#)] [[PubMed](#)]
18. Fan, Y. Study on Lower Limb Exoskeleton for Rehabilitation Based on Multi-Source Information Fusion Including SEMG & Interactive Force and Its Clinical Trail. Ph.D. Dissertation, Shanghai Jiao Tong University, Shanghai, China, 2014.
19. Artemiadis, P. EMG-Based Robot Control Interfaces: Past, Present and Future. *Adv. Robot. Autom.* **2012**, *1*, 1000e107. [[CrossRef](#)]
20. Lu, Z.; Chen, X.; Zhang, X.; Tong, K.-Y.; Zhou, P. Real-Time Control of an Exoskeleton Hand Robot with Myoelectric Pattern Recognition. *Int. J. Neur. Syst.* **2017**, *27*, 1750009. [[CrossRef](#)]
21. Secciani, N.; Topini, A.; Ridolfi, A.; Meli, E.; Allotta, B. A Novel Point-in-Polygon-Based SEMG Classifier for Hand Exoskeleton Systems. *IEEE Trans. Neural Syst. Rehabil. Eng.* **2020**, *28*, 3158–3166. [[CrossRef](#)]
22. Li, Z.; Wang, B.; Sun, F.; Yang, C.; Xie, Q.; Zhang, W. SEMG-Based Joint Force Control for an Upper-Limb Power-Assist Exoskeleton Robot. *IEEE J. Biomed. Health Inform.* **2014**, *18*, 1043–1050. [[CrossRef](#)]
23. Kiguchi, K.; Quan, Q. Muscle-Model-Oriented EMG-Based Control of an Upper-Limb Power-Assist Exoskeleton with a Neuro-Fuzzy Modifier. In Proceedings of the 2008 IEEE International Conference on Fuzzy Systems (IEEE World Congress on Computational Intelligence), Hong Kong, China, 1–6 June 2008; IEEE: Hong Kong, China, 2008; pp. 1179–1184.
24. Hagengruber, A.; Vogel, J. Functional Tasks Performed by People with Severe Muscular Atrophy Using an SEMG Controlled Robotic Manipulator. In Proceedings of the 2018 40th Annual International Conference of the IEEE Engineering in Medicine and Biology Society (EMBC), Honolulu, HI, USA, 18–21 July 2018; IEEE: Honolulu, HI, USA, 2018; pp. 1713–1718.

25. Vogel, J.; Hagengruber, A.; Iskandar, M.; Quere, G.; Leipscher, U.; Bustamante, S.; Dietrich, A.; Hoppner, H.; Leidner, D.; Albu-Schaffer, A. EDAN: An EMG-Controlled Daily Assistant to Help People With Physical Disabilities. In Proceedings of the 2020 IEEE/RSJ International Conference on Intelligent Robots and Systems (IROS), Las Vegas, NV, USA, 24 October 2020–24 January 2021; IEEE: Las Vegas, NV, USA, 2020; pp. 4183–4190.
26. Tamilselvi, R.; Merline, A.; Beham, M.P.; Anand, R.V.; Karthik, M.S.; Uthayakumar, R.H. EMG Activated Robotic Arm for Amputees. In Proceedings of the 2018 2nd International Conference on Inventive Systems and Control (ICISC), Coimbatore, India, 19–20 January 2018; IEEE: Coimbatore, India, 2018; pp. 456–461.
27. Al-Timemy, A.H.; Khushaba, R.N.; Bugmann, G.; Escudero, J. Improving the Performance Against Force Variation of EMG Controlled Multifunctional Upper-Limb Prostheses for Transradial Amputees. *IEEE Trans. Neural Syst. Rehabil. Eng.* **2016**, *24*, 650–661. [[CrossRef](#)]
28. Weitschat, R.; Dietrich, A.; Vogel, J. Online Motion Generation for Mirroring Human Arm Motion. In Proceedings of the 2016 IEEE International Conference on Robotics and Automation (ICRA), Stockholm, Sweden, 16–21 May 2016; IEEE: Stockholm, Sweden, 2016; pp. 4245–4250.
29. Hill, A.V. The Heat of Shortening and the Dynamic Constants of Muscle. *Proc. R. Soc. Lond. B* **1938**, *126*, 136–195. [[CrossRef](#)]
30. Holmes, J.W. Teaching from Classic Papers: Hill's Model of Muscle Contraction. *Adv. Physiol. Educ.* **2006**, *30*, 67–72. [[CrossRef](#)] [[PubMed](#)]
31. Morais, G.D.; Neves, L.C.; Masiero, A.A.; Castro, M.C.F. Application of Myo Armband System to Control a Robot Interface. In Proceedings of the 9th International Joint Conference on Biomedical Engineering Systems and Technologies, Rome, Italy, 21–23 February 2016; SCITEPRESS-Science and Technology Publications: Rome, Italy, 2016; pp. 227–231.
32. Atzori, M.; Gijssberts, A.; Kuzborskij, I.; Elsig, S.; Mittaz Hager, A.-G.; Deriaz, O.; Castellini, C.; Muller, H.; Caputo, B. Characterization of a Benchmark Database for Myoelectric Movement Classification. *IEEE Trans. Neural Syst. Rehabil. Eng.* **2015**, *23*, 73–83. [[CrossRef](#)] [[PubMed](#)]
33. Murillo, P.U.; Moreno, R.J.; Avilés, O. Individual Robotic Arms Manipulator Control Employing Electromyographic Signals Acquired by Myo Armbands. *Int. J. Appl. Eng. Res.* **2016**, *11*, 11241–11249.
34. Cheng, J.; Chen, X.; Shen, M. A Framework for Daily Activity Monitoring and Fall Detection Based on Surface Electromyography and Accelerometer Signals. *IEEE J. Biomed. Health Inform.* **2013**, *17*, 38–45. [[CrossRef](#)] [[PubMed](#)]
35. Grafakos, S.; Dimeas, F.; Aspragathos, N. Variable Admittance Control in PHRI Using EMG-Based Arm Muscles Co-Activation. In Proceedings of the 2016 IEEE International Conference on Systems, Man, and Cybernetics (SMC), Budapest, Hungary, 9–12 October 2016; IEEE: Budapest, Hungary, 2016; pp. 001900–001905.
36. Dost Sürücü, G.; Tezen, Ö. The Effect of EMG Biofeedback on Lower Extremity Functions in Hemiplegic Patients. *Acta Neurol. Belg.* **2021**, *121*, 113–118. [[CrossRef](#)]
37. Vogel, J.; Hagengruber, A. An SEMG-Based Interface to Give People with Severe Muscular Atrophy Control over Assistive Devices. In Proceedings of the 2018 40th Annual International Conference of the IEEE Engineering in Medicine and Biology Society (EMBC), Honolulu, HI, USA, 18–21 July 2018; IEEE: Honolulu, HI, USA, 2018; pp. 2136–2141.
38. Lu, Z.; Chen, X.; Li, Q.; Zhang, X.; Zhou, P. A Hand Gesture Recognition Framework and Wearable Gesture-Based Interaction Prototype for Mobile Devices. *IEEE Trans. Hum.-Mach. Syst.* **2014**, *44*, 293–299. [[CrossRef](#)]
39. Hao, S.; Wang, R.; Wang, Y.; Li, Y. A Spatial Attention Based Convolutional Neural Network for Gesture Recognition with HD-SEMG Signals. In Proceedings of the 2020 IEEE International Conference on E-health Networking, Application & Services (HEALTHCOM), Shenzhen, China, 1–2 March 2021; IEEE: Shenzhen, China, 2021; pp. 1–6.
40. Wu, J.; Sun, L.; Jafari, R. A Wearable System for Recognizing American Sign Language in Real-Time Using IMU and Surface EMG Sensors. *IEEE J. Biomed. Health Inform.* **2016**, *20*, 1281–1290. [[CrossRef](#)]
41. McManus, L.; Hu, X.; Rymer, W.Z.; Lowery, M.M.; Suresh, N.L. Changes in Motor Unit Behavior Following Isometric Fatigue of the First Dorsal Interosseous Muscle. *J. Neurophysiol.* **2015**, *113*, 3186–3196. [[CrossRef](#)] [[PubMed](#)]
42. Hu, X.L.; Tong, K.Y.; Wei, X.J.; Rong, W.; Susanto, E.A.; Ho, S.K. Coordinated Upper Limb Training Assisted with an Electromyography (EMG)-Driven Hand Robot after Stroke. In Proceedings of the 2013 35th Annual International Conference of the IEEE Engineering in Medicine and Biology Society (EMBC), Osaka, Japan, 3–7 July 2013; IEEE: Osaka, Japan, 2013; pp. 5903–5906.
43. Cote-Allard, U.; Fall, C.L.; Drouin, A.; Campeau-Lecours, A.; Gosselin, C.; Glette, K.; Laviolette, F.; Gosselin, B. Deep Learning for Electromyographic Hand Gesture Signal Classification Using Transfer Learning. *IEEE Trans. Neural Syst. Rehabil. Eng.* **2019**, *27*, 760–771. [[CrossRef](#)]
44. Bisi, S.; De Luca, L.; Shrestha, B.; Yang, Z.; Gandhi, V. Development of an EMG-Controlled Mobile Robot. *Robotics* **2018**, *7*, 36. [[CrossRef](#)]
45. Li, Z.; Zhao, X.; Liu, G.; Zhang, B.; Zhang, D.; Han, J. Electrode Shifts Estimation and Adaptive Correction for Improving Robustness of SEMG-Based Recognition. *IEEE J. Biomed. Health Inform.* **2021**, *25*, 1101–1110. [[CrossRef](#)] [[PubMed](#)]
46. Mao, L.; Yin, K.; Shen, J. Evaluation of SEMG Pattern Recognition: A Preliminary Study for Prostheses. In Proceedings of the 2021 IEEE 5th Advanced Information Technology, Electronic and Automation Control Conference (IAEAC), Chongqing, China, 12–14 March 2021; IEEE: Chongqing, China, 2021; pp. 955–959.
47. Suresh, N.; Li, X.; Zhou, P.; Rymer, W.Z. Examination of Motor Unit Control Properties in Stroke Survivors Using Surface EMG Decomposition: A Preliminary Report. In Proceedings of the 2011 Annual International Conference of the IEEE Engineering in Medicine and Biology Society, Boston, MA, USA, 30 August–3 September 2011; IEEE: Boston, MA, USA, 2011; pp. 8243–8246.

48. Meattini, R.; Benatti, S.; Scarcia, U.; Benini, L.; Melchiorri, C. Experimental Evaluation of a SEMG-Based Human-Robot Interface for Human-like Grasping Tasks. In Proceedings of the 2015 IEEE International Conference on Robotics and Biomimetics (ROBIO), Zhuhai, China, 6–9 December 2015; IEEE: Zhuhai, China, 2015; pp. 1030–1035.
49. Zeng, J.; Zhou, Y.; Yang, Y.; Yan, J.; Liu, H. Fatigue-Sensitivity Comparison of SEMG and A-Mode Ultrasound Based Hand Gesture Recognition. *IEEE J. Biomed. Health Inform.* **2022**, *26*, 1718–1725. [[CrossRef](#)] [[PubMed](#)]
50. Cene, V.; Tosin, M.; Machado, J.; Balbinot, A. Open Database for Accurate Upper-Limb Intent Detection Using Electromyography and Reliable Extreme Learning Machines. *Sensors* **2019**, *19*, 1864. [[CrossRef](#)] [[PubMed](#)]
51. Hochberg, L.R.; Bacher, D.; Jarosiewicz, B.; Masse, N.Y.; Simeral, J.D.; Vogel, J.; Haddadin, S.; Liu, J.; Cash, S.S.; van der Smagt, P.; et al. Reach and Grasp by People with Tetraplegia Using a Neurally Controlled Robotic Arm. *Nature* **2012**, *485*, 372–375. [[CrossRef](#)]
52. Chen, M.; Liu, H. Robot Arm Control Method Using Forearm EMG Signals. *MATEC Web Conf.* **2020**, *309*, 04007. [[CrossRef](#)]
53. Khan, A.M.; Khawaja, S.G.; Akram, M.U.; Khan, A.S. SEMG Dataset of Routine Activities. *Data Brief.* **2020**, *33*, 106543. [[CrossRef](#)]
54. Hassan, H.F.; Abou-Loukh, S.J.; Ibraheem, I.K. Teleoperated Robotic Arm Movement Using Electromyography Signal with Wearable Myo Armband. *J. King Saud. Univ.-Eng. Sci.* **2020**, *32*, 378–387. [[CrossRef](#)]
55. Atzori, M.; Muller, H. The Ninapro Database: A Resource for SEMG Naturally Controlled Robotic Hand Prosthetics. In Proceedings of the 2015 37th Annual International Conference of the IEEE Engineering in Medicine and Biology Society (EMBC), Milan, Italy, 25–29 August 2015; IEEE: Milan, Italy, 2015; pp. 7151–7154.
56. Liua, C.; Zhou, S.; Hu, S.; Wu, M. Hand Gesture Recognition Based on Semg Signal and Improved SVM Voting Method. In Proceedings of the 2020 IEEE 3rd International Conference on Information Systems and Computer Aided Education (ICISCAE), Dalian, China, 27–29 September 2020; IEEE: Dalian, China, 2020; pp. 605–608.
57. Fazeli, M.; Karimi, F.; Ramezani, V.; Jahanshahi, A.; Seyedin, S. Hand Motion Classification Using SEMG Signals Recorded from Dry and Wet Electrodes with Machine Learning. In Proceedings of the 2020 28th Iranian Conference on Electrical Engineering (ICEE), Tabriz, Iran, 4–6 August 2020; IEEE: Tabriz, Iran, 2020; pp. 1–4.
58. Hameed, H.K.; Hassan, W.Z.W.; Shafie, S.; Ahmad, S.A.; Jaafar, H.; Mat, L.N.I.; Alkubaisi, Y. Identifying the Best Forearm Muscle to Control Soft Robotic Glove System by Using a Single SEMG Channel. In Proceedings of the 2020 Advances in Science and Engineering Technology International Conferences (ASET), Dubai, United Arab Emirates, 4 February–9 April 2020; IEEE: Dubai, United Arab Emirates, 2020; pp. 1–4.
59. Zhang, Y.; Chen, Y.; Yu, H.; Yang, X.; Lu, W. Learning Effective Spatial–Temporal Features for SEMG Armband-Based Gesture Recognition. *IEEE Internet Things J.* **2020**, *7*, 6979–6992. [[CrossRef](#)]
60. Shenoy, P.; Miller, K.J.; Crawford, B.; Rao, R.P.N. Online Electromyographic Control of a Robotic Prosthesis. *IEEE Trans. Biomed. Eng.* **2008**, *55*, 1128–1135. [[CrossRef](#)]
61. Zhang, K.; Chen, F. Research on SEMG Gesture Recognition Based on Hybrid Dilated Convolutional Neural Network Combining Bidirectional Gated Recurrent Unit And Attention Mechanism. In Proceedings of the 2021 China Automation Congress (CAC), Beijing, China, 22–24 October 2021; IEEE: Beijing, China, 2021; pp. 3760–3763.
62. Wu, C.; Yan, Y.; Cao, Q.; Fei, F.; Yang, D.; Lu, X.; Xu, B.; Zeng, H.; Song, A. SEMG Measurement Position and Feature Optimization Strategy for Gesture Recognition Based on ANOVA and Neural Networks. *IEEE Access* **2020**, *8*, 56290–56299. [[CrossRef](#)]
63. Karheily, S.; Moukadem, A.; Courbot, J.-B.; Abdeslam, D.O. SEMG Time–Frequency Features for Hand Movements Classification. *Expert. Syst. Appl.* **2022**, *210*, 118282. [[CrossRef](#)]
64. Chen, R.; Chen, Y.; Guo, W.; Chen, C.; Wang, Z.; Yang, Y. SEMG-Based Gesture Recognition Using GRU With Strong Robustness Against Forearm Posture. In Proceedings of the 2021 IEEE International Conference on Real-time Computing and Robotics (RCAR), Xining, China, 15–19 July 2021; IEEE: Xining, China, 2021; pp. 275–280.
65. Duan, F.; Dai, L.; Chang, W.; Chen, Z.; Zhu, C.; Li, W. SEMG-Based Identification of Hand Motion Commands Using Wavelet Neural Network Combined With Discrete Wavelet Transform. *IEEE Trans. Ind. Electron.* **2016**, *63*, 1923–1934. [[CrossRef](#)]
66. Zhu, B.; Zhang, D.; Chu, Y.; Gu, Y.; Zhao, X. SeNic: An Open Source Dataset for SEMG-Based Gesture Recognition in Non-Ideal Conditions. *IEEE Trans. Neural Syst. Rehabil. Eng.* **2022**, *30*, 1252–1260. [[CrossRef](#)]
67. Chen, Z.; Yang, J.; Xie, H. Surface-Electromyography-Based Gesture Recognition Using a Multistream Fusion Strategy. *IEEE Access* **2021**, *9*, 50583–50592. [[CrossRef](#)]
68. Shen, C.; Pei, Z.; Chen, W.; Wang, J.; Zhang, J.; Chen, Z. Toward Generalization of SEMG-Based Pattern Recognition: A Novel Feature Extraction for Gesture Recognition. *IEEE Trans. Instrum. Meas.* **2022**, *71*, 1–12. [[CrossRef](#)]
69. Santiago, J.L.L.; Rios, P.; Arrustico, D.; Cortez, L. Volitional PD Computed Torque Control Design of a 2-DOF Finger Model for Cylindrical Grip Movement Assistance with SEMG Signal Classification. In Proceedings of the 2021 IEEE Engineering International Research Conference (EIRCON), Lima, Peru, 27–29 October 2021; IEEE: Lima, Peru, 2021; pp. 1–4.
70. Zhang, X.; Chen, X.; Zhao, Z.; Li, Q.; Yang, J.; Lantz, V.; Wang, K. An Adaptive Feature Extractor for Gesture SEMG Recognition. In *Medical Biometrics*; Zhang, D., Ed.; Lecture Notes in Computer Science; Springer: Berlin/Heidelberg, Germany, 2007; Volume 4901, pp. 83–90; ISBN 978-3-540-77410-5.
71. Kim, S.; Kim, M.; Lee, J.; Park, J. Robot Hand Synergy Mapping Using Multi-Factor Model and EMG Signal. In *Experimental Robotics*; Hsieh, M.A., Khatib, O., Kumar, V., Eds.; Springer Tracts in Advanced Robotics; Springer International Publishing: Cham, Switzerland, 2016; Volume 109, pp. 671–683; ISBN 978-3-319-23777-0.

72. Du, Y.; Jin, W.; Wei, W.; Hu, Y.; Geng, W. Surface EMG-Based Inter-Session Gesture Recognition Enhanced by Deep Domain Adaptation. *Sensors* **2017**, *17*, 458. [[CrossRef](#)]
73. Jarque-Bou, N.J.; Vergara, M.; Sancho-Bru, J.L.; Gracia-Ibáñez, V.; Roda-Sales, A. A Calibrated Database of Kinematics and EMG of the Forearm and Hand during Activities of Daily Living. *Sci. Data* **2019**, *6*, 270. [[CrossRef](#)]
74. Liu, B. Upper Limb Rehabilitation Training and Evaluation System Based on EEG and EMG Signals. Ph.D. Thesis, Zhengzhou University, Zhengzhou, China, 2020.
75. Li, Z. Parameterization of Human Upper Limb Movement Pattern and Its Application in Rehabilitation Robot. Ph.D. Thesis, Xinjiang University, Xinjiang, China, 2020.
76. Gopura, R.A.R.C.; Kiguchi, K. A Human Forearm and Wrist Motion Assist Exoskeleton Robot with EMG-Based Fuzzy-Neuro Control. In Proceedings of the 2008 2nd IEEE RAS & EMBS International Conference on Biomedical Robotics and Biomechanics, Scottsdale, AZ, USA, 19–22 October 2008; IEEE: Scottsdale, AZ, USA, 2008; pp. 550–555.
77. He, X.; Hao, M.; Wei, M.; Xiao, Q.; Lan, N. A Novel Experimental Method to Evaluate Motor Task Control in Parkinson's Patients. In Proceedings of the 2013 35th Annual International Conference of the IEEE Engineering in Medicine and Biology Society (EMBC), Osaka, Japan, 3–7 July 2013; IEEE: Osaka, Japan, 2013; pp. 6587–6590.
78. Maeda, Y.; Ishibashi, S. Operating Instruction Method Based on EMG for Omnidirectional Wheelchair Robot. In Proceedings of the 2017 Joint 17th World Congress of International Fuzzy Systems Association and 9th International Conference on Soft Computing and Intelligent Systems (IFSAS-SCIS), Otsu, Japan, 27–30 June 2017; IEEE: Otsu, Japan, 2017; pp. 1–5.
79. Bu, D.; Guo, S.; Li, H. SEMG-Based Motion Recognition of Upper Limb Rehabilitation Using the Improved Yolo-v4 Algorithm. *Life* **2022**, *12*, 64. [[CrossRef](#)]
80. Roy, S.H.; Cheng, M.S.; Chang, S.-S.; Moore, J.; De Luca, G.; Nawab, S.H.; De Luca, C.J. A Combined SEMG and Accelerometer System for Monitoring Functional Activity in Stroke. *IEEE Trans. Neural Syst. Rehabil. Eng.* **2009**, *17*, 585–594. [[CrossRef](#)]
81. Ding, Q.; Zhao, X.; Xiong, A.; Han, J. A Novel Motion Estimate Method of Human Joint with EMG-Driven Model. In Proceedings of the 2011 5th International Conference on Bioinformatics and Biomedical Engineering, Wuhan, China, 13–15 May 2011; IEEE: Wuhan, China, 2011; pp. 1–5.
82. Artemiadis, P.K.; Kyriakopoulos, K.J. An EMG-Based Robot Control Scheme Robust to Time-Varying EMG Signal Features. *IEEE Trans. Inform. Technol. Biomed.* **2010**, *14*, 582–588. [[CrossRef](#)]
83. Vogel, J.; Bayer, J.; van der Smagt, P. Continuous Robot Control Using Surface Electromyography of Atrophic Muscles. In Proceedings of the 2013 IEEE/RSJ International Conference on Intelligent Robots and Systems, Tokyo, Japan, 3–7 November 2013; IEEE: Tokyo, Japan, 2013; pp. 845–850.
84. Stillfried, G.; Stepper, J.; Nepl, H.; Vogel, J.; Höppner, H. Elastic Elements in a Wrist Prosthesis for Drumming Reduce Muscular Effort, but Increase Imprecision and Perceived Stress. *Front. Neurobot.* **2018**, *12*, 9. [[CrossRef](#)] [[PubMed](#)]
85. Abayasiri, R.A.M.; Jayasekara, A.G.B.P.; Gopura, R.A.R.C.; Kiguchi, K. EMG Based Controller for a Wheelchair with Robotic Manipulator. In Proceedings of the 2021 3rd International Conference on Electrical Engineering (EECon), Colombo, Sri Lanka, 24 September 2021; IEEE: Colombo, Sri Lanka, 2021; pp. 125–130.
86. Artemiadis, P.K.; Kyriakopoulos, K.J. EMG-Based Control of a Robot Arm Using Low-Dimensional Embeddings. *IEEE Trans. Robot.* **2010**, *26*, 393–398. [[CrossRef](#)]
87. Kiguchi, K.; Imada, Y.; Liyanage, M. EMG-Based Neuro-Fuzzy Control of a 4DOF Upper-Limb Power-Assist Exoskeleton. In Proceedings of the 2007 29th Annual International Conference of the IEEE Engineering in Medicine and Biology Society, Lyon, France, 22–26 August 2007; IEEE: Lyon, France, 2007; pp. 3040–3043.
88. Artemiadis, P.K.; Kyriakopoulos, K.J. Estimating Arm Motion and Force Using EMG Signals: On the Control of Exoskeletons. In Proceedings of the 2008 IEEE/RSJ International Conference on Intelligent Robots and Systems, Nice, France, 22–26 September 2008; IEEE: Nice, France, 2008; pp. 279–284.
89. Rojas-Martínez, M.; Serna, L.Y.; Jordanic, M.; Marateb, H.R.; Merletti, R.; Mañanas, M.Á. High-Density Surface Electromyography Signals during Isometric Contractions of Elbow Muscles of Healthy Humans. *Sci. Data* **2020**, *7*, 397. [[CrossRef](#)]
90. Rojas-Martínez, M.; Mañanas, M.A.; Alonso, J.F. High-Density Surface EMG Maps from Upper-Arm and Forearm Muscles. *J. Neuroeng. Rehabil.* **2012**, *9*, 85. [[CrossRef](#)] [[PubMed](#)]
91. Kiguchi, K. A Study on EMG-Based Human Motion Prediction for Power Assist Exoskeletons. In Proceedings of the 2007 International Symposium on Computational Intelligence in Robotics and Automation, Jacksonville, FL, USA, 20–22 June 2007; IEEE: Jacksonville, FL, USA, 2007; pp. 190–195.
92. De Baets, L.; Jaspers, E.; Janssens, L.; Van Deun, S. Characteristics of Neuromuscular Control of the Scapula after Stroke: A First Exploration. *Front. Hum. Neurosci.* **2014**, *8*, 933. [[CrossRef](#)] [[PubMed](#)]
93. Kiguchi, K.; Tanaka, T.; Fukuda, T. Neuro-Fuzzy Control of a Robotic Exoskeleton With EMG Signals. *IEEE Trans. Fuzzy Syst.* **2004**, *12*, 481–490. [[CrossRef](#)]
94. Lin, M.-W.; Ruan, S.-J.; Tu, Y.-W. A 3DCNN-LSTM Hybrid Framework for SEMG-Based Noises Recognition in Exercise. *IEEE Access* **2020**, *8*, 162982–162988. [[CrossRef](#)]
95. Luo, R.; Sun, S.; Zhang, X.; Tang, Z.; Wang, W. A Low-Cost End-to-End SEMG-Based Gait Sub-Phase Recognition System. *IEEE Trans. Neural Syst. Rehabil. Eng.* **2020**, *28*, 267–276. [[CrossRef](#)]

96. Li, C.; He, H.; Yin, S.; Deng, H.; Zhu, Y. Continuous Angle Prediction of Lower Limb Knee Joint Based on SEMG. In Proceedings of the 2021 IEEE International Conference on Recent Advances in Systems Science and Engineering (RASSE), Shanghai, China, 12–14 December 2021; IEEE: Shanghai, China, 2021; pp. 1–6.
97. Cai, C.; Yao, L.; Wei, X. ESECW Method to Process SEMG and Its Application in Gait Recognition. In Proceedings of the 2021 6th International Conference on Intelligent Computing and Signal Processing (ICSP), Xi'an, China, 9–11 April 2021; IEEE: Xi'an, China, 2021; pp. 525–528.
98. Khanjani, I.; Khoshdel, V.; Akbarzadeh, A. Estimate Human-Force from SEMG Signals for a Lower-Limb Rehabilitation Robot. In Proceedings of the 2017 Iranian Conference on Electrical Engineering (ICEE), Tehran, Iran, 2–4 May 2017; IEEE: Tehran, Iran, 2017; pp. 132–136.
99. Shi, X.; Qin, P.; Zhu, J.; Zhai, M.; Shi, W. Feature Extraction and Classification of Lower Limb Motion Based on SEMG Signals. *IEEE Access* **2020**, *8*, 132882–132892. [[CrossRef](#)]
100. De Luca, C.J.; Kuznetsov, M.; Gilmore, L.D.; Roy, S.H. Inter-Electrode Spacing of Surface EMG Sensors: Reduction of Crosstalk Contamination during Voluntary Contractions. *J. Biomech.* **2012**, *45*, 555–561. [[CrossRef](#)]
101. Stock, M.S.; Beck, T.W.; Defreitas, J.M. Effects of Fatigue on Motor Unit Firing Rate versus Recruitment Threshold Relationships: Motor Unit Fatigue. *Muscle Nerve* **2012**, *45*, 100–109. [[CrossRef](#)]
102. Roy, S.H.; De Luca, G.; Cheng, M.S.; Johansson, A.; Gilmore, L.D.; De Luca, C.J. Electro-Mechanical Stability of Surface EMG Sensors. *Med. Bio Eng. Comput.* **2007**, *45*, 447–457. [[CrossRef](#)]
103. De Luca, C.J.; Donald Gilmore, L.; Kuznetsov, M.; Roy, S.H. Filtering the Surface EMG Signal: Movement Artifact and Baseline Noise Contamination. *J. Biomech.* **2010**, *43*, 1573–1579. [[CrossRef](#)] [[PubMed](#)]
104. De Luca, C.J.; Merletti, R. Surface Myoelectric Signal Cross-Talk among Muscles of the Leg. *Electroencephalogr. Clin. Neurophysiol.* **1988**, *69*, 568–575. [[CrossRef](#)] [[PubMed](#)]
105. Beck, T.W.; DeFreitas, J.M.; Stock, M.S. The Effects of a Resistance Training Program on Average Motor Unit Firing Rates. *Clin. Kinesiol.* **2011**, *9*.
106. Nawab, S.H.; Chang, S.-S.; De Luca, C.J. High-Yield Decomposition of Surface EMG Signals. *Clin. Neurophysiol.* **2010**, *121*, 1602–1615. [[CrossRef](#)] [[PubMed](#)]
107. Zaheer, F.; Roy, S.H.; De Luca, C.J. Preferred Sensor Sites for Surface EMG Signal Decomposition. *Physiol. Meas.* **2012**, *33*, 195–206. [[CrossRef](#)]
108. Beck, T.W.; Kasishke, P.R.; Stock, M.S.; DeFreitas, J.M. Eccentric Exercise Does Not Affect Common Drive in the Biceps Brachii: Muscle Damage and Common Drive. *Muscle Nerve* **2012**, *46*, 759–766. [[CrossRef](#)]
109. Defreitas, J.M.; Beck, T.W.; Ye, X.; Stock, M.S. Synchronization of Low- and High-Threshold Motor Units: Synchronization of Low- and High-Threshold Motor Units. *Muscle Nerve* **2014**, *49*, 575–583. [[CrossRef](#)]
110. Roy, S.H.; De Luca, C.J.; Schneider, J. Effects of Electrode Location on Myoelectric Conduction Velocity and Median Frequency Estimates. *J. Appl. Physiol.* **1986**, *61*, 1510–1517. [[CrossRef](#)]
111. Kline, J.C.; De Luca, C.J. Error Reduction in EMG Signal Decomposition. *J. Neurophysiol.* **2014**, *112*, 2718–2728. [[CrossRef](#)]
112. Kuan, J.-Y.; Huang, T.-H.; Huang, H.-P. Human Intention Estimation Method for a New Compliant Rehabilitation and Assistive Robot. In Proceedings of the SICE Annual Conference 2010, Taipei, Taiwan, 18–21 August 2010; pp. 2348–2353.
113. Schiel, F.; Hagengruber, A.; Vogel, J.; Triebel, R. Incremental Learning of EMG-Based Control Commands Using Gaussian Processes. In Proceedings of the 2020 Conference on Robot Learning, Virtual, 16–18 November 2020; pp. 1137–1146.
114. Al-Faiz, M.Z.; Miry, A.H. Artificial Human Arm Driven by EMG Signal. In *MATLAB—A Fundamental Tool for Scientific Computing and Engineering Applications—Volume 1*; Katsikis, V., Ed.; IntechOpen: London, UK, 2012; ISBN 978-953-51-0750-7.
115. Al-Timemy, A.H.; Bugmann, G.; Escudero, J.; Outram, N. Classification of Finger Movements for the Dexterous Hand Prosthesis Control With Surface Electromyography. *IEEE J. Biomed. Health Inform.* **2013**, *17*, 608–618. [[CrossRef](#)] [[PubMed](#)]
116. Phinyomark, A.; Quaine, F.; Charbonnier, S.; Serviere, C.; Tarpin-Bernard, F.; Laurillau, Y. EMG Feature Evaluation for Improving Myoelectric Pattern Recognition Robustness. *Expert. Syst. Appl.* **2013**, *40*, 4832–4840. [[CrossRef](#)]
117. Kiguchi, K.; Tamura, K.; Hayashi, Y. Estimation of Joint Force/Torque Based on EMG Signals. In Proceedings of the 2013 IEEE Workshop on Robotic Intelligence in Informationally Structured Space (RiiSS), Singapore, 16–19 April 2013; IEEE: Singapore, 2013; pp. 20–24.
118. Wang, J.-Y.; Dai, Y.-H.; Si, X.-X. Feature Layer Fusion of Linear Features and Empirical Mode Decomposition of Human EMG Signal. *J. Electron. Sci. Technol.* **2022**, *20*, 100169. [[CrossRef](#)]
119. Shen, S.; Wang, X.; Mao, F.; Sun, L.; Gu, M. Movements Classification Through SEMG With Convolutional Vision Transformer and Stacking Ensemble Learning. *IEEE Sens. J.* **2022**, *22*, 13318–13325. [[CrossRef](#)]
120. Zhang, X.; Zhou, P. Sample Entropy Analysis of Surface EMG for Improved Muscle Activity Onset Detection against Spurious Background Spikes. *J. Electromyogr. Kinesiol.* **2012**, *22*, 901–907. [[CrossRef](#)]
121. Hudgins, B.; Parker, P.; Scott, R.N. A New Strategy for Multifunction Myoelectric Control. *IEEE Trans. Biomed. Eng.* **1993**, *40*, 82–94. [[CrossRef](#)]
122. Farrell, T.R.; Weir, R.F. The Optimal Controller Delay for Myoelectric Prostheses. *IEEE Trans. Neural Syst. Rehabil. Eng.* **2007**, *15*, 111–118. [[CrossRef](#)]

123. Smith, L.H.; Hargrove, L.J.; Lock, B.A.; Kuiken, T.A. Determining the Optimal Window Length for Pattern Recognition-Based Myoelectric Control: Balancing the Competing Effects of Classification Error and Controller Delay. *IEEE Trans. Neural Syst. Rehabil. Eng.* **2011**, *19*, 186–192. [[CrossRef](#)]
124. Rahimian, E.; Zabihi, S.; Atashzar, S.F.; Asif, A.; Mohammadi, A. XceptionTime: A Novel Deep Architecture Based on Depthwise Separable Convolutions for Hand Gesture Classification. *arXiv* **2019**, arXiv:1911.03803.
125. Atzori, M.; Gijssberts, A.; Castellini, C.; Caputo, B.; Hager, A.-G.M.; Elsig, S.; Giatsidis, G.; Bassetto, F.; Müller, H. Electromyography Data for Non-Invasive Naturally-Controlled Robotic Hand Prostheses. *Sci. Data* **2014**, *1*, 140053. [[CrossRef](#)] [[PubMed](#)]
126. Li, Z.; Huang, Z.; He, W.; Su, C.-Y. Adaptive Impedance Control for an Upper Limb Robotic Exoskeleton Using Biological Signals. *IEEE Trans. Ind. Electron.* **2017**, *64*, 1664–1674. [[CrossRef](#)]
127. Minati, L.; Yoshimura, N.; Koike, Y. Hybrid Control of a Vision-Guided Robot Arm by EOG, EMG, EEG Biosignals and Head Movement Acquired via a Consumer-Grade Wearable Device. *IEEE Access* **2016**, *4*, 9528–9541. [[CrossRef](#)]
128. Jain, R.K.; Datta, S.; Majumder, S. Biomimetic Behavior of IPMC Using EMG Signal for Micro Robot. *Mech. Based Des. Struct. Mach.* **2014**, *42*, 398–417. [[CrossRef](#)]
129. Gowtham, S.; Krishna, K.M.A.; Srinivas, T.; Raj, R.G.P.; Joshuva, A. EMG-Based Control of a 5 DOF Robotic Manipulator. In Proceedings of the 2020 International Conference on Wireless Communications Signal Processing and Networking (WiSPNET), Chennai, India, 4–6 August 2020; IEEE: Chennai, India, 2020; pp. 52–57.

Disclaimer/Publisher’s Note: The statements, opinions and data contained in all publications are solely those of the individual author(s) and contributor(s) and not of MDPI and/or the editor(s). MDPI and/or the editor(s) disclaim responsibility for any injury to people or property resulting from any ideas, methods, instructions or products referred to in the content.